Theory on quench-induced pattern formation: Application to the isotropic to smectic-*A* phase transitions

Zhou Haijun[1,*] and Ou-Yang Zhong-can[1,2]
[1]*Institute of Theoretical Physics, Chinese Academy of Sciences, P.O. Box 2735, Beijing 100080, China*
[2]*Center for Advanced Study, Tsinghua University, Beijing 100084, China*
(Received 8 May 1998)

During catastrophic processes of environmental variations of a thermodynamic system, such as rapid temperature decrease, many different and complex patterns often form. To understand such phenomena, a general mechanism is proposed based on the competition between heat transfer and conversion of heat to other energy forms. We apply it to the smectic-*A* filament growth process during the quench-induced isotropic to smectic-*A* phase transition. Analytical forms for the buckling patterns are derived and we find good agreement with experimental observation [H. Naito, M. Okuda, and Ou-Yang Zhong-can, Phys. Rev. E **55**, 1655 (1997)]. The present work strongly indicates that rapid cooling will lead to structural transitions in the smectic-*A* filament at the molecular level to optimize heat conversion. The force associated with this pattern formation process is estimated to be on the order of 10^{-1} pN. [S1063-651X(98)04311-6]

PACS number(s): 64.70.Md, 62.20.Fe, 46.30.Lx, 05.70.−a

When a thermodynamic system in some initial stable phase is subjected to rapid or abrupt environmental variations such as decreased temperature and varied ionic conditions, many different patterns will often form. For example, in volcanic eruptions streams of lava spurt out and cool rapidly, during which many tensile bubbles are spontaneously formed and the lava becomes a porous material [1,2]. Similar bubbles and strips are seen in supercooled biomembranes [3]. In the rapid growth process of carbon nanotubes initial straight tubes are observed to change into regular helical shapes, even at fixed environmental conditions [4]. Other puzzling phenomena include the kink instabilities of short DNA rings in solution: On adding some specific ions, a circular ring changes abruptly into a polygonal ring [5].

All these transitions and pattern formations are radically different from those slow, quasistatic processes discussed in conventional textbooks, such as the isothermal solid-liquid transitions. In the solidification process of water, for example, the transition takes place very slowly and at any time during this process solid and liquid phases can be regarded as in equilibrium with each other and with the environment, the bulk temperature is kept constant, and latent heat of transition is released. However, for those catastrophic processes mentioned above [1–5], the quasistatic and quasiequilibrium assumptions are no longer satisfied, since the system is now far away from equilibrium and changes rapidly over time [6]. Therefore, we have to create different ways and insights to properly understand them. A deep understanding of such phenomena is needed both for its own sake and for various practical purposes, such as the optimal growth conditions for some important materials. In recent years much research effort has been devoted to this field [6–10]. For example, in Refs. [6] and [7] (and in other references) the spinodal decomposition and formation of separate patterns in a binary mixture are studied both theoretically and experimentally using, respectively, linear stability analysis and x-ray-scattering technique. References [8–10,6] have investigated the solid-liquid interphase patterns during directional solidification processes induced by a large temperature gradient. A very important aspect of the mechanism for these pattern formation phenomena is that the pattern formation is controlled mainly by the relatively slow diffusive transport process of heat energy out of the system [6]. Thus it seems that this mechanism cannot give a satisfactory explanation of those pattern formation processes mentioned in the first paragraph of this paper. This is partly because of the fact that in these systems the effects of other energy forms become comparable to that of heat energy [1–5] and they are expected to play a significant role in determining the patterns formed.

In this paper we try to understand the nature of these rapid pattern formation processes by regarding them as quenchlike processes induced by, say, decreasing temperature. Our main reasoning is as follows. In a quench process caused by rapid cooling, the thermal energy or heat of the system must be evacuated as quickly as possible. However, this demand cannot be met just through the relatively slow heat exchange process occurring at the system surface and a great part of the thermal energy is thus expected to be converted into other energy forms [11,12], mechanical, elastic, and maybe even *electromagnetic*, which can accommodate a large amount of energy quickly and efficiently. Therefore, during the quench process, because of the competition between heat transfer and heat conversion, the structures of the system, both at macroscopic level and at molecular level, might change dramatically and many different and complex patterns are expected to form spontaneously. It resembles in some sense the rapid expansion of ideal gases, which is regarded as an adiabatic process since the system has no time to exchange heat with the environment.

To check the validity of this perspective and show how to implement it in actual practice, we investigate a specific phe-

*Electronic address: zhouhj@itp.ac.cn

nomenon based on this insight, namely, the growth and pattern formation process of smectic-*A* (Sm-*A*) filaments from an isotropic (*I*) liquid phase induced by rapid cooling [13]. Although the subject is quite specific, the general reasoning is the same and can be applied to many other pattern formation processes. Our theoretical results show that on cooling, an initial straight filament will buckle and take on some specific kind of curved configuration, which can be well described by elliptic integrals. Good agreement with the experiment of Ref. [14] has been attained, indicating the usefulness and robustness of our treatment. As also speculated in Ref. [14], the present work confirms that structural transitions in the Sm-*A* filament at the molecular level are required in order to optimize heat conversion. The force associated with this pattern formation is also discussed in this paper.

As observed in the *I*-Sm-*A* phase transition process [14], at the initial stage, thin, hollow, and straight Sm-*A* liquid-crystalline tubes appear from the *I* phase on cooling. As the temperature is further decreased, these straight filaments buckle at the growing ends and take on somewhat complex serpentine forms, the amplitudes of which become larger and larger. The filaments are metastable and eventually transform to compact domains after the filaments become extremely convoluted. Although this transition phenomenon seems to be very complex, we found that its physics is actually simple and the patterns formed can be well described by analytical functions.

As we have known, the net difference in the energy between a thin Sm-*A* filament and the *I* phase is the sum of the following three terms [13,14]: (i) the volume free-energy change due to the *I*-Sm-*A* transition $F_V=-g_0V=-\pi(\rho_o^2-\rho_i^2)\int g_0 ds$, where g_0 is the difference in the Gibbs free-energy densities between *I* and Sm-*A* phases and *V* is the volume of the Sm-*A* nucleus, ρ_o and ρ_i are, respectively, the outer and inner radii of the Sm-*A* microtube, and *s* is the arc length along the central line **r** of it; (ii) the surface energy of the outer and inner Sm-*A*-*I* interfaces $F_A=\gamma(A_o+A_i)=2\pi(\rho_o+\rho_i)\gamma\int ds$, where γ is the Sm-*A*-*I* interfacial tension and A_o and A_i are the surface areas of the outer and inner surfaces, respectively; and (iii) the curvature elastic energy of the Sm-*A* filament

$$F_c=(k_{11}/2)\int(\nabla\cdot\mathbf{N})^2dV+(2k_{11}+k_5)(\rho_o-\rho_i)\oint K\,dA_i$$
$$=k_c\int\kappa(s)^2ds+\pi k_{11}\ln(\rho_o/\rho_i)\int ds,$$

where k_{ij} is the Oseen-Frank elastic constants, $k_5=2k_{13}-k_{22}-k_{24}$, $k_c=\pi k_{11}(\rho_o^2-\rho_i^2)/4$, **N** and *K* are, respectively, the director and Gaussian curvature defined on the inner surface of the Sm-*A* tube, and κ is the curvature defined along **r** [14,15].

The total energy difference is thus $F=F_V+F_A+F_c=k_c\int\kappa(s)^2+\int(\lambda+\sqcap)ds$, where $\lambda=\pi k_{11}\ln(\rho_o/\rho_i)+2\pi\gamma(\rho_o+\rho_i)$ and $\sqcap=-\pi g_0(\rho_o^2-\rho_i^2)$ [14]. We call *F* the *shape formation energy* of the Sm-*A* filament. The variation equation $\delta F=0$ yields the equilibrium-shape equation of the filament:

$$k_c(\kappa^3-2\kappa\tau^2+2\ddot{\kappa})-(\lambda+\sqcap)\kappa=0, \tag{1}$$

$$4\dot{\kappa}\tau+2\kappa\dot{\tau}=0, \tag{2}$$

where τ is the torsion of the filament's central line **r**, according to the Frenet formula [16]; overdots and double overdots mean, respectively, the first- and second-order differentiations with respect to the arc length *s*.

It is obvious that a straight line is always a solution of the above equation since $\kappa=\tau=0$. The corresponding shape formation energy of a straight filament is $F=(\lambda+\sqcap)l$, where *l* is the length of the straight filament. In the rapid cooling process, it is impossible to effectively transfer redundant heat out of the system by means of heat exchange with the environment and a Sm-*A* straight filament will form spontaneously and quickly to partly accommodate the redundant energy, *as long as* $\lambda+\sqcap>0$. Straight Sm-*A* filaments have been observed to form at the initial stage of the growth process [14]. However, since the value of g_0 increases with decreasing temperature [14,17], while γ exhibits no temperature dependence or a weak one [18], $\lambda+\sqcap$ will decrease with cooling and the equilibrium threshold condition of $F=0$ yields the criteria for the growth of a straight filament as

$$\pi k_{11}\ln(\rho_o/\rho_i)+2\pi\gamma(\rho_o+\rho_i)-\pi g_0(\rho_o^2-\rho_i^2)=0, \tag{3}$$

beyond which forming a straight filament will no longer help absorb thermal energy. This situation is unfavorable to the quench process and consequently the resultant remnant part of the energy will prevent the straight filament from remaining stable. Then a shape deformation will be induced, which would lead to another solution of the shape equation to convert as much of the thermal energy into elastic deformation energy as possible. In other words, the straight filament will buckle to a curved configuration where, *on the one hand,* κ *and* τ *should satisfy Eqs.* (1) *and* (2) *so the new pattern will be stable and, on the other hand, the stable new configuration should be capable of absorbing as much thermal energy as possible*. Then, to what configurations will the filament deform?

Now we will prove that the observed Sm-*A* serpentine planar patterns shown in Ref. [14] are just the allowed solutions of Eqs. (1) and (2). For the convenience of comparison with experimentally observed planar curved patterns, we will confine ourselves to the planar case, where $\tau=0$. Then Eq. (2) is automatically satisfied and Eq. (1) reduces to

$$k_c(\kappa^4+2\kappa\ddot{\kappa})-(\lambda+\sqcap)\kappa^2=0, \tag{4}$$

where we have multiplied both sides of Eq. (1) by κ. We define the filament's tangential unit vector to be $\mathbf{t}(s)=(\cos\phi(s),\sin\phi(s),0)$; then $\kappa^2=\dot{\phi}^2$. Inserting this into Eq. (4), we know that ϕ is determined by

$$\dot{\phi}^2=-2\eta+\frac{f}{k_c}\cos(\phi-\phi_0), \tag{5}$$

where $\eta=-(\lambda+\sqcap)/2k_c$ [14], *f* is a positive constant (later we will show that *f* is actually the mean repulsive force exerted on the growing end of the filament), and ϕ_0 is an

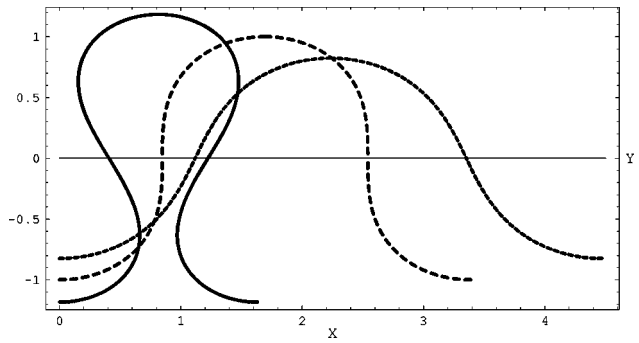

FIG. 1. Shapes of one period of the buckled patterns [Eq. (8)] for $m=0.339\,175$ (dotted line), $m=0.5$ (dashed line), and $m=0.7$ (solid line). The length unit is set to be $\sqrt{2k_c/f}$.

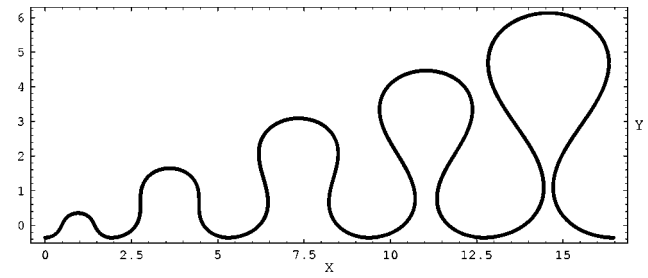

FIG. 2. Simulated buckling filament shape during the growth process. Segments formed later have longer period arc length and larger amplitude, caused by increased values of k_{11}. The unit length is set to be $\sqrt{2k_c^i/f}$, where k_c^i is the value of k_c at the onset of buckling.

integration constant. The solution of Eq. (5) is a periodic function and its form in the range $\phi\in[0,\arccos(1-2m)]$ is expressed as [19]

$$\sqrt{\frac{2k_c}{f}}F\left(\arcsin\sqrt{\frac{1-\cos\phi}{2m}},\sqrt{m}\right)=s-s_0, \tag{6}$$

where

$$m=\frac{1}{2}-\frac{k_c\eta}{f}\in(0,1), \tag{7}$$

s_0 is another integration constant, and $F(\psi,k)$ is the first kind of elliptic integral. In the same range the filament shape is determined, up to an additive constant vector, by [19]

$$\mathbf{r}(s)=\sqrt{\frac{2k_c}{f}}\left[2E\left(\arcsin\sqrt{\frac{1-\cos\phi}{2m}},\sqrt{m}\right)-F\left(\arcsin\sqrt{\frac{1-\cos\phi}{2m}},\sqrt{m}\right),-\sqrt{2m+\cos\phi-1}\right], \tag{8}$$

where $E(\psi,k)$ is the second kind of elliptic integral. The trajectory of the filament in the whole range can also be obtained easily from Eqs. (5), (6), and (8). The general shapes are shown in Fig. 1 in the cases of $m<1/2$ or $\eta>0$ (dotted curve), $m=1/2$ or $\eta=0$ (dashed curve), and $m>1/2$ or $\eta<0$ (solid curve) for one period of the trajectory. The total arc length of each period is calculated to be [19]

$$P=4\sqrt{\frac{2k_c}{f}}K(\sqrt{m}) \tag{9}$$

and the shape formation energy density of each period is [19]

$$\chi=\frac{1}{P}\int_0^P(k_c\dot{\phi}^2-2\eta)ds=f[2L(\sqrt{m})-3+4m], \tag{10}$$

where $K(k)$ and $E(k)$ are, respectively, the first and the second kind of complete elliptic integral, and $L(\sqrt{m})=E(\sqrt{m})/K(\sqrt{m})$.

At the initial stage of buckling, the filament will deform to a configuration to make the threshold condition $\chi=0$ be satisfied, which leads to $m=m_i=0.339\,175$ at this stage. The corresponding deformed shape is the dotted curve of Fig. 1, which is very similar to the observed initial buckling shape Ref. [14] [see Figs. 1(b) and 1(c) therein]. Furthermore, for this shape, the amplitude of the deformation is calculated to be $Y_{max}=\sqrt{4mk_c/f}$ from Eq. (8) and the distance traversed along the growth direction for one-half of the trajectory period is $X_{max}=\sqrt{2k_c/f}[2E(\sqrt{m})+K(\sqrt{m})]$, thus $Y_{max}/X_{max}=0.737$ for the above-mentioned value of m_i. On the experimental side, we can estimate the values of this ratio to be, respectively, about 0.85 and 0.64 from Figs. 1(c) and 1(d) of Ref. [14] and the mean value is 0.745, all in close agreement with the theoretical value.

As mentioned before, after buckling, the filament will ''try its best'' to adjust its structures to accommodate thermal energy. Differentiating χ in Eq. (10) with respect to m, we find that the maximum value of the shape formation energy density χ is reached at the point where $m_o=0.9689$ and in the range between m_i and m_o, χ is a continuously increasing function of m. Thus, after the buckling process has been triggered, m will try to increase from its initial value m_i, until the value m_o is reached. Since m is determined by Eq. (7), we anticipated that $\lambda+\sqcap$ will change from a negative value (and hence $m<1/2$) to zero ($m=1/2$) and then become more and more positive ($m>1/2$). The question is how this can be achieved by the Sm-*A* filament.

We know that g_0 increases with decreasing temperature, γ exhibits little temperature dependence, and during the cooling process there are no significant changes in the filament radii ρ_o and ρ_i, therefore, the only possible reason accounting for $\lambda+\sqcap$ changing from negative to positive values is that k_{11}, the quantity related to the molecular structures of Sm-*A* filaments, rapidly increases its value. In other words, quench may induce some structural transition in the Sm-*A* filament at the molecular level. (In Ref. [14] it is speculated that such a transition is the *trans* to *cis* transition

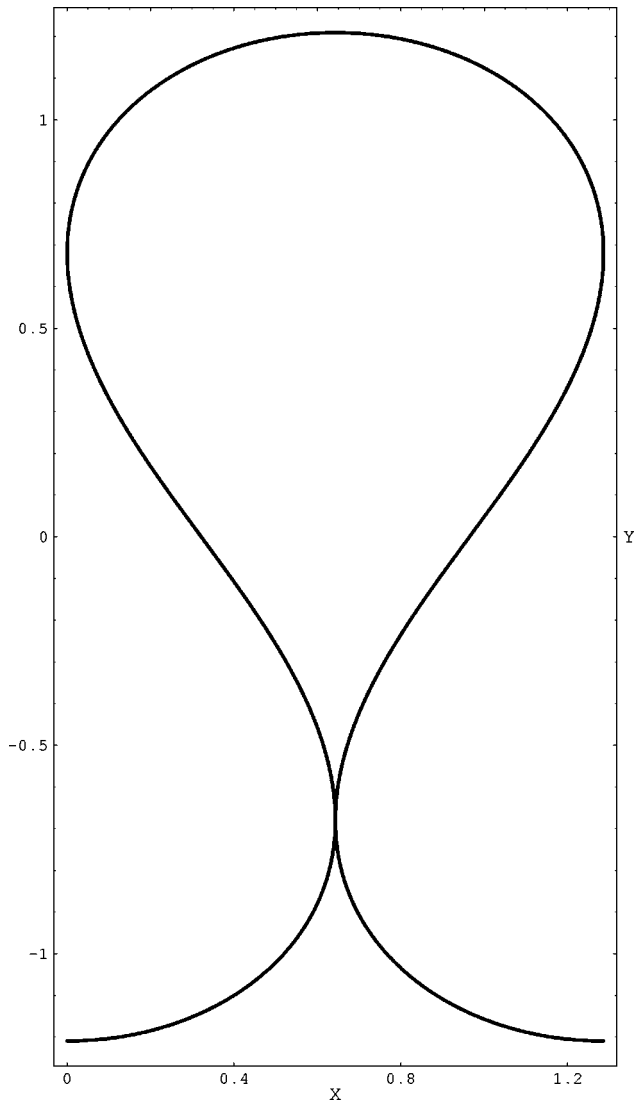

FIG. 3. Onset of self-intersection of the buckled pattern at $m=0.731\,183$. The appearance of self-intersections might trigger the transition from filament structures to compact domains. The length unit is the same as in Fig. 1.

occurring in the alkyl chains of the Sm-*A* liquid crystal material. Further experimental observations are still needed in this respect.) Consequently, the initial curved pattern will take the form demonstrated by the dotted curve in Fig. 1, segments formed later will take the form of the dashed curve, and segments formed still later will be the form of the solid curve. This trend is demonstrated more clearly in Fig. 2. A buckled pattern resembling that of Fig. 2 has indeed been observed and recorded in the experiment of Ref. [14] [see Fig. 1 of [14], in particular Fig. 1(d)], showing the correctness of the pattern formation mechanism based on the competition between heat transfer and heat conversion.

When m is increased to the value $m_c=0.731\,183<m_o$, different segments of the same filament begin to intersect, as shown in Fig. 3. At this stage, the formed serpentine patterns may begin to collapse because of possible strong contacting forces and eventually the filament will transform to compact domains [14]. Thus actually the optimal value m_o cannot be reached by the system.

So far we have not discussed the physical meaning of the parameter f in Eq. (5). Now we begin to investigate this question. Our result is that f is actually the mean repulsive force exerted on the filament growing end. There has been clear experimental evidence that both the assembly and disassembly of microtubular filaments can generate force; however, only limited quantitative data are available on the actual magnitude of these forces [20]. In the case of Sm-*A* filaments discussed here, we estimate the force exerted on the ends to be on the order of 10^{-1} pN. This magnitude is reasonable, as indicated by various experiments on thin filaments [20,21]. The forces associated with the assembly and disassembly of filaments may be of vital biological significance. For example, it has long been speculated that the motion of chromosomes during mitosis of the cell cycle is caused by the assembly and disassembly of cytoskeletal microtubes [20].

To show that the parameter f in Eq. (5) corresponds to the average force exerted at the ends, we will rederive Eq. (5), the stable planar shape equation, in another way. The already grown Sm-*A* filament can be viewed as an inextensible string. When subjected to the constraint of a fixed end-to-end distance, the total shape energy is expressed as $F=\int[k_c\dot{\mathbf{t}}^2+\lambda+\sqcap-\mathbf{f}\cdot\mathbf{t}]ds$, with $\mathbf{t}(s)=(\sin\theta\cos\phi,\sin\theta\sin\phi,\cos\theta)$ being the string direction vector; here $\mathbf{f}$ is a Lagrange multiplier corresponding to this constraint, which, according to thermodynamic principles, is just the average force exerted by the environment on the filament ends. The first variation $\delta F=0$ leads to the shape equation expressed in terms of θ, ϕ and their differentiations with respect to s. For our planar case with $\theta=\pi/2$, the nonstraight stable configurations are found to be determined by

$$\dot{\phi}^2=C+\frac{|\mathbf{f}|}{k_c}\cos(\phi-\phi_0'+\pi), \tag{11}$$

where ϕ_0' is the angle between the x axis and the direction of the average force $\mathbf{f}$. From Eq. (11) we know that the filament's tangential direction (growth direction) $\mathbf{t}$ is on average antiparallel to $\mathbf{f}$, therefore $\mathbf{f}$ must be a repulsive force. Comparing Eq. (11) with Eq. (5), we can obviously infer that the parameter f in Eq. (5) is just the magnitude of the average force $\mathbf{f}$ and $C=-2\eta$ in Eq. (11). This force is induced by thermal current and we have assumed it to be constant throughout the growth process.

The magnitude of the force can also be estimated from the buckling amplitude of the filament. As mentioned before, the deformation amplitude $Y_{max}=\sqrt{4mk_c/f}$, therefore $f=4mk_c/Y_{max}^2$. At the initial stage of buckling, $m=m_i=0.339\,175$, we take $k_{11}=10^{-6}$ dyn according to Ref. [13], and estimate that $\rho_o=1.3$ μm, $\rho_i=0.8$ μm, and $Y_{max}=10.4$ μm from Fig. 1(c) of Ref. [14]. Thus the average repulsive force is calculated to be $f\simeq1.4\times10^{-13}$ N or 0.14 pN. It is interesting to note that the forces related to polymeric strings are often on the order of 10^{-2}–10^{1} pN [20,21].

In summary, in this paper we have proposed a theory to explain the different pattern formation phenomena induced by catastrophic variations of environmental temperature or other parameters. We then applied this general insight to the

understanding of the pattern formation process of smectic-A filaments grown from an isotropic liquid phase. Exact buckling patterns have been obtained and compared with experiment and we achieved excellent agreement with experiment. We also suggested that decreasing temperature leads to some structural transitions at the molecular level for the Sm-*A* filament, possibly the *trans* to *cis* transition of the alkyl chains of the material used in the experiment of [14]. The force associated with the pattern formation process of smectic-A filaments is estimated to be on the order of 0.1 pN.

One of the authors (Z.H.) appreciates valuable discussions with Dr. Yan Jie, Dr. Liu Quanhui, and Dr. Zhao Wei. This work was partly supported by the National Natural Science Foundation of China.

[1] G. Debrégeas, P.-G. de Gennes, and F. Brochard-wyart, Science **279**, 1704 (1998).
[2] M. T. Mangau and K. V. Cashman, J. Volcanol. Geotherm. Res. **73**, 1 (1996).
[3] J. F. Tocanne, P. H. J. Th. Ververgaert, A. J. Verkleij, and L. L. M. van Deenen, Chem. Phys. Lipids **12**, 220 (1974); B. Sternberg, J. Gumpert, G. Reinhardt, and K. Gawrisch, Biochim. Biophys. Acta **898**, 223 (1987); H. W. Meyer, W. Richter, and J. Gumpert, *ibid.* **1026**, 171 (1990).
[4] X. B. Zhang *et al.*, Europhys. Lett. **27**, 141 (1994).
[5] Wenhai Han, S. M. Lindsay, M. Dlakic, and R. E. Harrington, Nature (London) **386**, 563 (1997).
[6] *Solids Far From Equilibrium*, edited by G. Godrèche (Cambridge University Press, Cambridge, 1991).
[7] A. E. Bailey and D. S. Cannell, Phys. Rev. Lett. **70**, 2110 (1993).
[8] J. S. Langer, Rev. Mod. Phys. **52**, 1 (1980).
[9] J. A. Warren and J. S. Langer, Phys. Rev. A **42**, 3518 (1990); Phys. Rev. E **47**, 2702 (1998).
[10] W. Losert, B. Q. Shi, and H. Z. Cummins, Proc. Natl. Acad. Sci. USA **95**, 431 (1998); **95**, 439 (1998).
[11] Ou-Yang Zhong-can, Z.-B. Su, and C.-L. Wang, Phys. Rev. Lett. **78**, 4055 (1997).
[12] Yan Jie, Zhou Haijun, and Ou-Yang Zhong-can, Mod. Phys. Lett. B **12**, 147 (1998).
[13] H. Naito, M. Okuda, and Ou-Yang Zhong-can, Phys. Rev. Lett. **70**, 2912 (1993); Phys. Rev. E **52**, 2095 (1995), and references therein.
[14] H. Naito, M. Okuda, and Ou-Yang Zhong-can, Phys. Rev. E **55**, 1655 (1997).
[15] W. Helfrich, Z. Naturforsch. C **28**, 693 (1973); Ou-Yang Zhong-can, S. Liu, and Xie Yu-zhang, Mol. Cryst. Liq. Cryst. **204**, 143 (1991).
[16] M. P. do Carmo, *Differential Geometry of Curves and Surfaces* (Prentice-Hall, Englewood Cliffs, NJ, 1976).
[17] N. J. Chou, S. W. Depp, J. M. Eldrige, M. H. Lee, G. J. Sprokel, A. Juliana, and J. Brown, J. Appl. Phys. **54**, 1827 (1983).
[18] R. Pratibha and N. V. Madhusudana, J. Phys. II **2**, 383 (1992).
[19] P. E. Byrd and M. D. Friedman, *Handbook of Elliptic Integrals for Engineers and Physicists* (Springer-Verlag, Berlin, 1954).
[20] M. Dogterom and B. Yurke, Science **278**, 856 (1997), and references therein.
[21] S. B. Smith, L. Finzi, and C. Bustamante, Science **258**, 1122 (1992); C. Bustmante, J. Marko, E. Siggia, and S. Smith, *ibid.* **265**, 1599 (1994); E. W. Wong, P. E. Sheehan, and C. M. Lieber, *ibid.* **277**, 1971 (1997).